Orientation of 1-Butyl-3-methylimidazolium Based Ionic Liquids at a Hydrophobic Quartz Interface Using Sum Frequency Generation Spectroscopy

ARTICLE *in* THE JOURNAL OF PHYSICAL CHEMISTRY C · NOVEMBER 2006

Impact Factor: 4.77 · DOI: 10.1021/jp0640225

4 AUTHORS, INCLUDING:

Henry Justin Moore
University of Texas Rio Grande Valley
10 PUBLICATIONS **178** CITATIONS

SEE PROFILE

Orientation of 1-Butyl-3-methylimidazolium Based Ionic Liquids at a Hydrophobic Quartz Interface Using Sum Frequency Generation Spectroscopy

Casey Romero, H. Justin Moore, T. Randall Lee, and Steven Baldelli*

Department of Chemistry, University of Houston, Houston, Texas 77204-5003

Received: June 27, 2006; In Final Form: October 9, 2006

The room-temperature ionic liquid/hydrophobic quartz interface was examined using sum frequency generation vibrational spectroscopy in the C−H stretching region to develop a more detailed model of how ionic liquids absorb to a variety of solid surfaces. Deuterated dodecyltrichlorosilane was synthesized to modify the quartz surface, which produced a hydrophobic quartz interface that had no resonances from C−H stretches. The ionic liquids, 1-butyl-3-methylimidazolium tetrafluoroborate [BMIM][BF_4] and 1-butyl-3-methylimidazolium hexafluorophosphate [BMIM][PF_6], and neutral derivatives, 1-methylimidazole and 1-butylimidazole, were used in the analysis. The neutral molecules were examined to compare how shape and charge influenced the orientation of the ionic liquids at a hydrophobic interface. The methyl groups of the four compounds studied were oriented much closer to the surface normal than on the hydrophilic quartz surface. This suggested that the methyl groups were arranged toward the alkylsilane monolayer. The sum frequency generation (SFG) spectra suggest that the imidazolium rings of the ionic liquids are lying in the plane of the interface. Ionic liquids at three different interfaces—air/liquid, hydrophobic quartz/liquid, and hydrophilic quartz/liquid—were compared.

Introduction

Room-temperature ionic liquids (RTILs) have become a widely studied class of compounds within the past decade because of their unique properties. They are composed completely of ions and are liquid at room temperature. One of the most interesting characteristics of ionic liquids is the ability to tune their physical properties by changing the structure/identity of the cation or anion. Properties such as the melting point, density, viscosity, and water miscibility are affected by changing the length of the alkyl chain on the cation or by changing the anion.[1] While the bulk properties of RTILs have been widely studied, the interfacial structure has only been examined in a few studies.[2−11] In a previous study, sum frequency generation (SFG) spectroscopy was used to examine the RTILs/quartz interface. It was concluded that both the anion and the cation were adsorbed to the quartz surface and that the size of the anion influenced the orientation of the cation.[12] To develop a more complete model of how ionic liquids absorb to a variety of solid surfaces, the RTIL/hydrophobic quartz interface was examined. The simplest procedure used to create a hydrophobic quartz surface is to graft a layer of hydrocarbon or fluorocarbon chains onto the quartz surface through self-assembly by the reaction of an alkyl-trichlorosilane ($RSiCl_3$) molecule.[13,14] This reaction involves the trichlorosilyl head group to react with the hydroxyls on the substrate surface to form siloxy bonds. When R is a long-chain alkane, this produces an organic monolayer that is highly ordered, hydrophobic, and chemically and physically stable.[15] The drawback to using this method is that well-ordered alkylsilane monolayers produce a large amount of SFG signal.[14−16] Thus, the vibrational resonances of ionic liquids adsorbed to the surface appear as only small contributions to the SFG signal produced from the interface. This problem was overcome by using a totally deuterated dodecyltrichlorosilane $CD_3(CD_2)_{11}SiCl_3$ to create the hydrophobic monolayer. This created a hydrophobic monolayer which was free of C−H vibrations. Therefore, all vibrations within the C−H stretching region (2800−3300 cm^{-1}) can be assigned to vibrations from the adsorbed molecules without interference from the hydrophobic monolayer.

Sum Frequency Generation. Sum frequency generation spectroscopy was used for this study because of its ability to probe buried interfaces to detect a monolayer in the presence of a large number of bulk molecules. SFG is second-order nonlinear process which only occurs in media without inversion symmetry. This allows for SFG to be sensitive only at interfaces where the bulk centrosymmetry is broken. In SFG vibrational spectroscopy, a tunable infrared laser beam and a fixed visible beam are used to obtain the vibrational spectra at the sum frequency of the molecular groups at an interface. The SFG intensity is proportional to the intensities of the incident laser beams and the square of the sum frequency susceptibility, $|\chi^{(2)}|^2$.

$$I \approx |\chi^{(2)}|^2 E_{vis}{}^2 E_{IR}{}^2 \quad (1)$$

$\chi^{(2)}$contains the measurable information on the response of the molecular system to the incident electric fields. The sum frequency susceptibility contains contributions from each of the resonant vibrations, $\chi_R^{(2)}$, as well as contributions that are not dependent on the infrared frequency, called nonresonant contributions, $\chi_{NR}^{(2)}$.

$$\chi^{(2)} = \chi_{NR}{}^{(2)} + \sum \chi_R{}^{(2)} \quad (2)$$

The resonant portion of the sum frequency susceptibility is enhanced when the frequency of the incident infrared beam, ω_{IR}, is in resonance with an SFG active vibrational mode. Only vibrational modes that are both IR and Raman active will produce resonant SFG signal.

* To whom correspondence should be addressed. E-mail: SBaldelli@uh.edu.

10.1021/jp0640225 CCC: $37.00
Published on Web 11/21/2006

$$\chi_R^{(2)} = \frac{A}{\omega_{IR} - \omega_q + i\Gamma} \quad (3)$$

where A is the amplitude of the resonance, ω_q is the frequency of the q^{th} vibrational mode, and Γ is the damping constant. $\chi_R^{(2)}$ is a macroscopic quantity that can be related to the microscopic properties of the interface through the following relation.

$$\chi_R^{(2)} = N\langle\beta\rangle \quad (4)$$

where N is the number of molecules contributing to the signal and $\langle\beta\rangle$ is the molecular hyperpolarizability tensor orientationally averaged. This not only shows that SFG signal is a function of the types of molecules that are at the interface but also how the molecules are oriented. This unique aspect of SFG spectroscopy allows for the ability to determine the orientation of molecular groups at an interface.[17−20]

Experimental

Sum Frequency Generation Spectrometer Setup. The details of the SFG spectrometer used in this study have been described elsewhere.[2] A picosecond pulsed Nd:YAG (Ekspla) laser was used as the fundamental (1064 nm) to pump an optical parametric generator (OPG) (LaserVision). The OPG produced an infrared beam which was tunable between 2000 cm^{-1} and 4000 cm^{-1} as well as a fixed visible beam (532 nm). The beams were aligned in a co-propagating configuration with the visible and infrared beams incident at 50° and 60° from normal, respectively. The SFG signal emitted was filtered from the incident visible using optical filters and was passed through a linear polarizer to select polarization state. The SFG signal was then passed through a $\lambda/4$ waveplate to produce circular polarized light. This was done to prevent differences in grating efficiency for s and p polarized light when passing through the monochromator which was used as a filter. The filtered SFG signal was then detected with a photomultiplier tube and was analyzed by a gated integrator. A computer program created in LabVIEW was used to collect the signal from the gated integrator and to scan the infrared frequency. The infrared frequency was scanned at 1 cm^{-1}/s. Fluctuations in infrared intensity were accounted for by normalizing spectra with a background spectrum from gold.

Synthesis of $CD_3(CD_2)_{11}SiCl_3$. Deuterated dodecyltrichlorosilane ($CD_3(CD_2)_{11}SiCl_3$ or d-DTS) was synthesized from $C_{12}D_{25}Br$ purchased from Cambridge Isotope Laboratories, Inc according to the following reactions.[21]

$$CD_3(CD_2)_{11}Br + Mg^\circ \xrightarrow[\text{reflux 30 min}]{\text{ether}} CD_3(CD_2)_{11}MgBr$$

$$CD_3(CD_2)_{11}MgBr + SiCl_4 \xrightarrow{\text{ether}} CD_3(CD_2)_{11}SiCl_3$$

Silicon tetrachloride was purchased from Sigma-Aldrich and was used as received. Diethyl ether was purchased from EM Science and was distilled at 40 °C under argon gas prior to use. Magnesium turnings were purchased from Sigma-Aldrich.

Freshly ground magnesium turnings, 0.44 g (0.183 mol), were placed in a 100-mL 3-neck round-bottom flask (rbf) fitted with a 50-mL addition funnel, a magnetic stir bar, and a reflux condenser. The entire apparatus was sealed and flame-dried under a flow of argon to remove any moisture. Dry diethyl ether (∼3 mL) was added to the reflux apparatus via cannula (insertion tube) to cover the magnesium. In a separate sealed and flame-dried 50-mL rbf was placed 1.0 g (3.65 mmol) of $C_{12}D_{25}Br$. About 25 mL of dry diethyl ether was also added to the flask containing $C_{12}D_{25}Br$ via cannula. This solution was then transferred to the addition funnel of the reflux apparatus. Two to three drops of 1,2-dibromoethane were directly added to the ether/magnesium mixture via syringe to initiate the Grignard reaction. At the first signs of ethylene gas evolution, the bromide/ether solution was added slowly to maintain a gentle reflux. After the addition was complete, the reaction was refluxed at 80 °C for ∼30 min.

After allowing the reaction to cool to room temperature, the Grignard reagent was transferred via cannula to a sealed, flame-dried, and air-free glass frit filter apparatus. The Grignard reagent was pulled through the glass filter by suction into a Schlenk flask to remove any excess, unreacted magnesium.

To a 100-mL rbf equipped with a 50-mL addition funnel and magnetic stir bar was added 2.48 g (14.6 mmol) of $SiCl_4$. The $SiCl_4$ was diluted with ∼20 mL of dry diethyl ether. The Grignard reagent previously prepared was transferred to the addition funnel and was added slowly over a period of 1.5 h to the vigorously stirred $SiCl_4$ solution. The reaction was left to stir for 12 h at room temperature. After stirring for 12 h, a white precipitate formed that was removed by filtering through glass wool.

The excess $SiCl_4$ and ether were removed by simple distillation. The remaining residue (∼5 mL) was washed with ether and was transferred to a homemade trap-to-trap vacuum distillation apparatus. The residue/ether solution was placed in a trap partially filled with glass beads to prevent bumping when the apparatus was evacuated to remove the ether. After all of the ether was removed, the residue was heated under vacuum (∼30 mTorr) with a methane torch. The clear liquid was collected in a tube in a liquid-nitrogen-cooled trap and was sealed using a glass-blowing hand torch with an O_2/CH_4 fuel mixture. This procedure produced 1−1.5 mL of deuterated dodecyltrichlorosilane.

Preparation of Deuterated Silane Monolayer. A fused IR quartz equilateral prism (ISP optics) was used as the substrate for silane deposition. The prism was cleaned by soaking in 1:1 (v/v) mixture of concentrated H_2SO_4/HNO_3 overnight and then was rinsed repetitively using water from a Millipore A10 system (18.2 MΩ cm). The cleaned prism was then rinsed with methanol (Aldrich spectrophotometric grade 99.9+%) and was placed in anhydrous heptane (Aldrich 99%) to remove water from the surface. The deuterated silane solution was prepared by dissolving 0.5 mL of deuterated dodecyltrichlorosilane in 100 mL of anhydrous heptane. The solution was sonicated for 5 min before the prism was introduced. The prism was then placed in the silane solution for 2 h in order for the silane monolayer to form. After deposition of deuterated silane monolayer, the prism was rinsed repeatedly with heptane.

Quartz Surface Characterization. Contact angle measurements were performed on the modified prism to ensure hydrophobicity. Static contact angles were measured using an automated analyzer with a CCD camera (KSV Instruments Ltd., CAM 200), fitted with drop shape analysis software, which was used to determine the angle between the surface and the 8−15 μL drops of Nanopure water. SFG spectroscopy, within the C−D stretching region 2000−2300 cm^{-1}, was also performed on the modified prism to ensure the formation of the deuterated alkylsilane monolayer (Figure 1). The C−H stretching region, 2800−3300 cm^{-1}, was also examined to ensure that there were no resonances from the deuterated silane monolayer or surface contamination.

Sample Preparation. The same ionic liquids and neutral derivatives used in the previous study were used in the analysis.

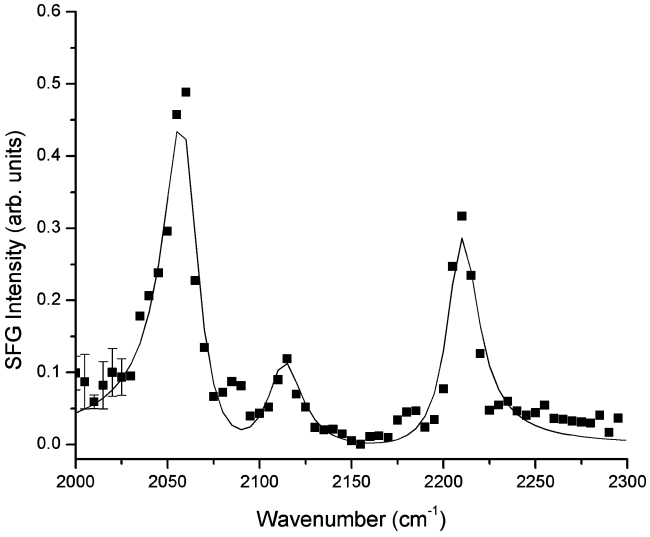

Figure 1. SFG spectra of deuterated silane monolayer modified prism surface: ssp polarization combination.

1-Butyl-3-methylimidazolium tetrafluoroborate [BMIM][BF_4] and 1-butyl-3-methylimidazolium hexafluorophosphate [BMIM]-[PF_6] were synthesized in our laboratory by a procedure outlined previously.[4] 1-Methylimidazole was purchased from Aldrich and was used as received. 1-Butylimidazole was purchased from Aldrich and was distilled before use. The cell used for these experiments was made entirely out of glass with a Kalrez O-ring between the cell and the prism used as the window. The cell was cleaned by soaking in 1:1 (v/v) H_2SO_4/HNO_3 solution overnight and was rinsed repetitively with Millipore water. After characterization, the silane-modified quartz prism was rinsed with methanol and was attached to the cell. Two different preparation methods were used, depending on the compound being studied. For the ionic liquids, the cell was attached to a vacuum line and was pumped down to $<3 \times 10^{-5}$ Torr. The ionic liquids, [BMIM][BF_4] and [BMIM][PF_6], were pumped down to $<3 \times 10^{-5}$ Torr and were backfilled with dry argon gas before addition to the cell to remove any trace amounts of water. Because 1-methylimidazole and 1-butylimidazole have much higher vapor pressures than the ionic liquids, the cell was dried by flowing ultrahigh purity nitrogen through the cell for 15 min before filling with either of the neutral molecules.

Results

Modified Quartz Surface. The static water contact angle measured for the modified quartz prism was 97° ± 2°. This value is consistent with the literature for trichloroalkylsilanes on silicon.[22] ssp polarized SFG spectra of the deuterated silane-modified prism were performed in the C−D stretching region (2000−2300 cm^{-1}) and are shown in Figure 1. The spectrum has three resonances from the symmetric methyl stretch, Fermi resonance, and antisymmetric methyl stretch at 2059 cm^{-1}, 2113 cm^{-1}, and 2209 cm^{-1}. The frequencies are consistent with literature values of *n*-alkanes determined from infrared spectroscopy.[23] The absence of methylene resonances is evidence of a well-ordered monolayer free of gauche defects, and thus the hydrocarbon chains are largely trans-extended.[20] SFG spectra of the C−H stretching region (2800−3300 cm^{-1}) was also performed to ensure that the silane monolayer contained no C−H contributions and to make certain that there was no surface contamination.

SFG Spectra. SFG spectroscopy was performed on the four compounds of interest using three polarization combinations ssp, ppp, and sps from 2800 to 3300 cm^{-1}. The data presented here are an average of five scans of the infrared frequency over the desired range. All spectra were fit using eq 2 and these fits are shown as the solid lines in Figures 2−5. In a previous work, polarized Raman spectroscopy was performed on each of the four compounds studied and these results were used to designate peak assignments.[12] The spectra are drastically different from the hydrophilic quartz interface. The same vibrational modes are visible but thier relative intensities are different. The other major difference was the sps polarized spectra. For the hydrophilic quartz interface, there were no visible resonances in the sps spectra. The appearance of the antisymmetric methyl stretch in the sps spectra is believed to be due to the orientation of the methyl groups being much closer to being aligned with the surface normal than on the hydrophilic quartz surface.[24] This will be discussed in a following section.

1-Methylimidazole. SFG spectra of the 1-methylimidazole/hydrophobic quartz interface are shown in Figure 2. The ssp polarization combination (Figure 2A) was fit with seven peaks. The methyl symmetric, Fermi resonance, and antisymmetric vibrational modes were at 2952 cm^{-1}, 2912 cm^{-1}, and 3010 cm^{-1}, respectively. The vibrations at 3109 cm^{-1} and 3135 cm^{-1} are from the antisymmetric and symmetric H−C(4)C(5)−H stretches of the imidazole ring. The vibration at 3070 cm^{-1} is due to the CH vibration of the C2 carbon of the imidazole ring. There is also a combination band at 2814 cm^{-1}.[25,26] The ppp polarization combination (Figure 2B) contains the same resonances as the ssp spectra. The only resonances visible in the sps polarization combination (Figure 2C) are the antisymmetric methyl stretch at 3010 cm^{-1}, the antisymmetric H−C(4)C(5)−H stretch at 3109 cm^{-1} from the imidazole ring, and a small contribution from the symmetric H−C(4)C(5)−H stretch from the imidazole ring at 3135 cm^{-1}.

1-Butylimidazole. The SFG spectra of the 1-butylimidazole/hydrophobic quartz interface are shown in Figure 3. The ssp spectrum (Figure 3A) was fit with three peaks at 2867 cm^{-1}, 2934 cm^{-1}, and 2963 cm^{-1} assigned symmetric, Fermi resonance, and antisymmetric modes from the methyl group. There is also a resonance at 3130 cm^{-1} from the symmetric H−C(4)C-(5)−H stretch from the imidazole ring. The ppp polarization combination (Figure 3B) contains the same three vibrations from the methyl group, whereas the contribution from the imidazole ring is the antisymmetric H−C(4)C(5)−H stretch at 3112 cm^{-1}. The sps polarized spectra (Figure 3C) was fit with only two contributions from the antisymmetric methyl stretch at 2965 cm^{-1} and the asymmetric ring mode at 3112 cm^{-1}.

1-Butyl-3-methylimidazolium Tetrafluoroborate. SFG spectra of the [BMIM][BF_4]/hydrophobic quartz interface are shown in Figure 4. The ssp polarization combination (Figure 4A) was fit with five resonances. The three largest contributions at 2874 cm^{-1}, 2936 cm^{-1}, and 2965 cm^{-1} are from the symmetric, Fermi resonance, and antisymmetric modes of the methyl group at the end of the butyl chain. There are also much weaker contributions from the C−H stretch from the C2 carbon of the imidazolium ring at 3130 cm^{-1} and the antisymmetric H−C(4)C(5)−H stretch at 3155 cm^{-1}. The ppp polarized spectra contain the same three resonances from the methyl group at the end of the butyl chain with the antisymmetric mode having much more intensity than the symmetric mode. The antisymmetric ring mode and the C−H stretch from the C2 carbon on the imidazolium ring are also visible in the spectra. The only peak that is apparent in the ppp polarized spectra and not in the ssp spectra is the antisymmetric methylene vibration at 2913 cm^{-1}. The only

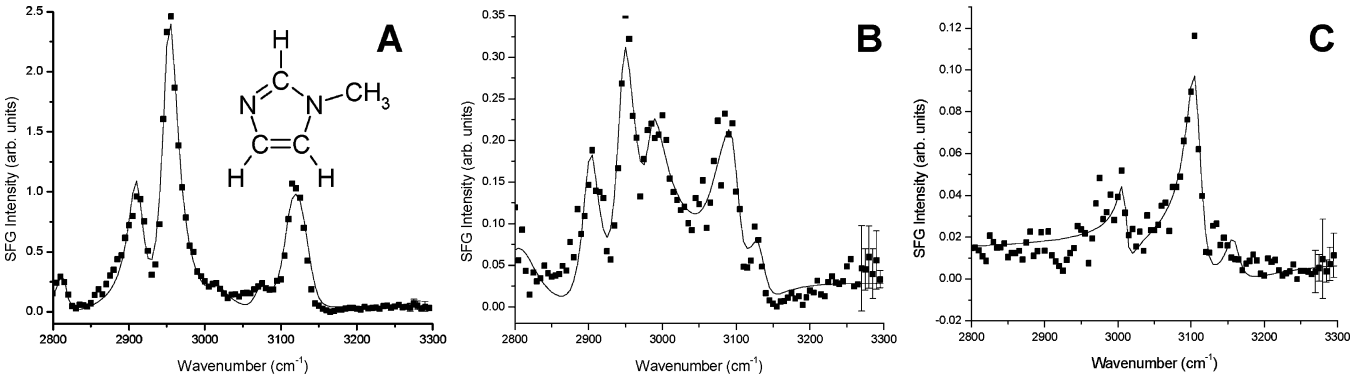

Figure 2. SFG spectra of 1-methylimidazole/modified quartz interface with fit (A) ssp, (B) ppp, and (C) sps polarization combination.

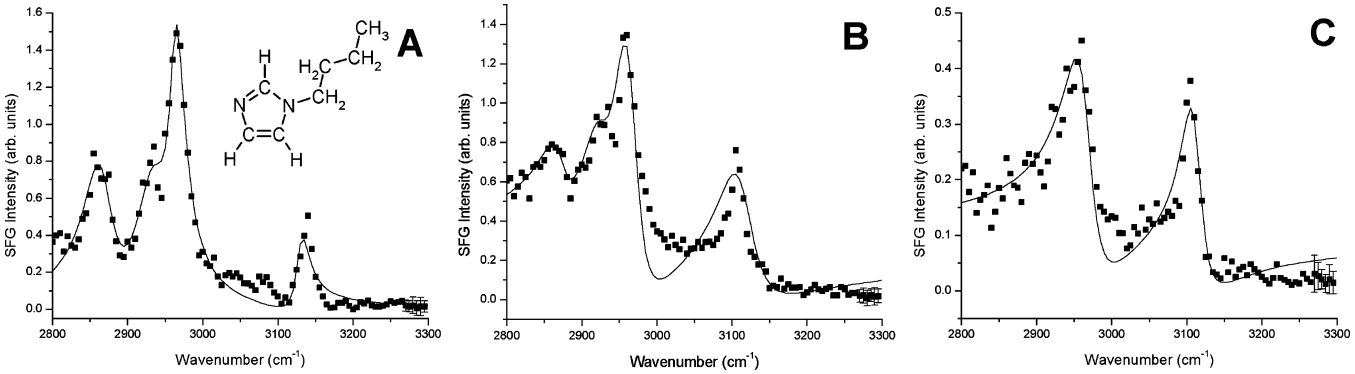

Figure 3. SFG spectra of 1-butylimidazole/modified quartz interface with fit (A) ssp, (B) ppp, and (C) sps polarization combination.

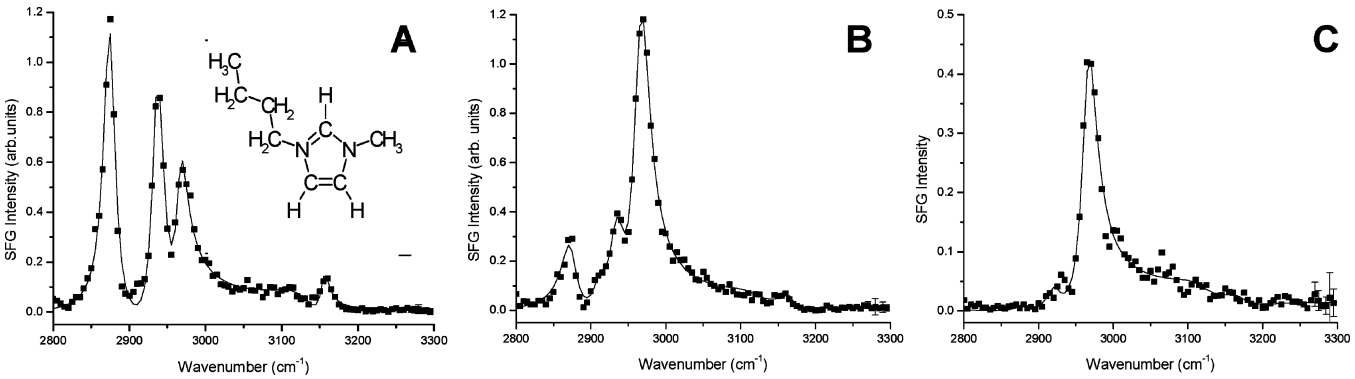

Figure 4. SFG spectra of 1-butyl-3-methylimidazolium [BF_4]/modified quartz interface with fit (A) ssp, (B) ppp, and (C) sps polarization combination.

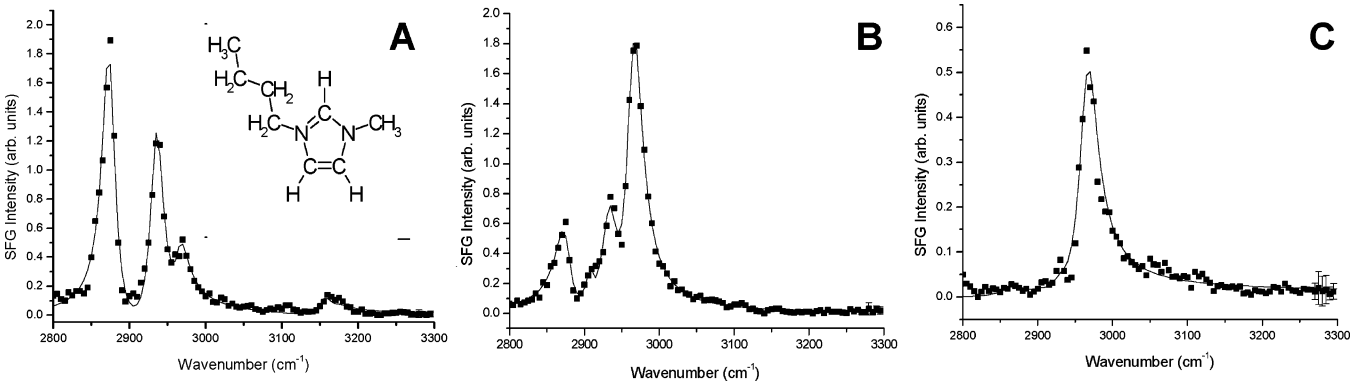

Figure 5. SFG spectra of 1-butyl-3-methylimidazolium [PF_6]/modified quartz interface with fit (A) ssp, (B) ppp, and (C) sps polarization combination.

substantial resonance in the sps polarized spectra was the antisymmetric methyl stretch at 2965 cm^{-1}.

1-Butyl-3-methylimidazolium Hexafluorophosphate. The SFG spectra of the [BMIM][PF_6]/hydrophobic quartz interface (Figure 5) are similar to the [BMIM][BF_4] spectra. The three strongest resonances are assigned to the symmetric, Fermi resonance, and antisymmetric methyl stretches at 2874 cm^{-1}, 2935 cm^{-1}, and 2965 cm^{-1}, respectively. The antisymmetric methyl stretch of [BMIM][PF_6] is smaller than for the [BMIM]-[BF_4]/hydrophobic quartz interface in the ssp polarized spectra (Figure 5A). Both the symmetric and antisymmetric H−C(4)C-(5)−H ring stretches are discernible in the spectra at 3174 cm^{-1}

and 3154 cm^{-1}, respectively. The ppp polarized spectra (Figure 5B) only has contributions from the alkyl chain. As with the [BMIM][BF_4] interface, the three methyl stretches and the antisymmetric methylene stretch are observable. The sps (Figure 5C) polarized spectrum only contains one significant resonance from the antisymmetric methyl stretch.

Orientation Analysis. It is possible to gain information on the polar ordering of a molecular group using polarization-dependent SFG spectroscopy to probe different tensor elements of the surface susceptibility.[20,27,28] Orientation information is usually determined by comparing the ratios of peak intensities with a calculated theoretical orientation curve. When intensity ratios of different polarization combinations are analyzed, differences in the local fields must be taken into account.

To relate the macroscopic SFG susceptibility, $\chi_{ijk}^{(2)}$, to the microscopic hyperpolarizability, β_{abc}, a coordinate transformation is performed.[18,28−30] The components of the transformation matrix depend on the Euler angles (θ, ϕ, χ), which relate the molecular and laboratory-fixed coordinate systems. The tilt angle, θ, is defined at zero degrees when normal to the interface. The twist angle, ϕ, which is along the molecular axis, is defined at zero degrees in plane with the interface. χ is the azimuthal angle around the plane of the interface. The two point groups that will be examined in this manuscript are C_{3v} (methyl group) and C_{2v} (ring stretch). After calculating the Fresnel coefficients, hyperpolarizability tensors, and integrating the equations determined from the coordinate transformation, the resulting equations are plotted as a function of the orientation of the molecular group. Ratios of experimental intensities of the molecular vibrations are then plotted against the theoretical curves (Figures 6−8), and their overlap determines the orientation of the functional group. A delta function distribution was assumed for all systems studied.

Each SFG spectra shown was fit using eq 3 with an instrumental weighting method which took into account scatter in the data as well as fitting error. The coefficients given from each of the fits have a standard deviation associated with them. To correctly determine how much effect the error of each coefficient has on the orientation calculation, a rigorous error analysis was performed. Each peak has three coefficients, A, the amplitude of the peak, Γ, the damping constant (or width of the peak), and, ω_q, which is the frequency of the peak. To correctly compare the intensities of resonances, the amplitudes of each peak were divided by their widths (normalized) and were squared.[31,32]

$$I = \left(\frac{A}{\Gamma}\right)^2 \tag{5}$$

When performing mathematical operations on values with a standard deviation, a more detailed mathematical operation must be performed.[33] Since each parameter has an associated standard deviation, these all must be taken into account to get a true representation of the error.[33]

A more detailed description of the orientation analysis used in this work can be found in a previous work (or in the Supporting Information) which describes the orientation calculation for the molecules studied at a hydrophilic quartz interface.[12] The only difference, for orientation calculation purposes, for the hydrophilic system and the hydrophobic system was the change in the refractive index of the monolayer. The refractive index of dodecyltrichlorosilane (1.46) is similar to the refractive index used for the monolayer in the previous study (1.49). This small change did not affect the theoretical orientation curves. Thus, the orientation calculation used in this work was kept identical to the method used in the previous work on the hydrophilic quartz surface.[12] Although these curves are limited for the absolute orientation analysis, they are useful for comparison, as in this work. The ratios of the ssp symmetric and antisymmetric methyl stretching intensities as a function of tilt angle are shown in Figure 6. The tilt angle of the methyl group for each of the molecules studied for both the hydrophilic and the hydrophobic quartz interfaces is shown in Table 1. For each of the molecules studied, the tilt angle of the methyl group is much closer to normal for the hydrophobic surface than for the hydrophilic quartz interface.[12] This is believed to be due to the alkyl chain of the molecule orienting with the alkyl chain of the silane monolayer. This arrangement is similar to the orientation of lipid bilayers[34−36] and polymer interfaces.[37] The hydrophobic head groups of the alkylsilane and the butyl chain of the ionic liquid are arranged with the methyl groups facing each other.

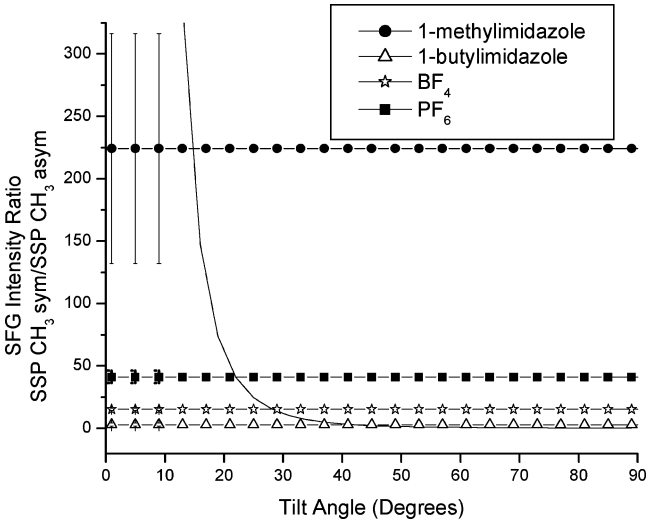

Figure 6. Simulation of SFG signal as a function of methyl group orientation of liquid/modified quartz interface.

TABLE 1: Orientation of Methyl Group and Cation Ring from Surface Normal for Hydrophilic and Hydrophobic Quartz Interface[a]

	hydrophilic quartz		hydrophobic quartz	
	methyl	ring (twist)	methyl	ring (twist)
1-methylimidazole	32−35	45−68 (0−30)	13−17	35−90 (0−40)
1-butylimidazole	43−47	70−90 (0−10)	≥40	31−82 (0−50)
[BMIM][BF_4]	78−90	45−90 (0−30)	27−29	70−90 (0−10)
[BMIM][PF_6]	58−64	38−58 (0−30)	21−24	60−90 (0−20)

[a] All values are in degrees.

On the hydrophilic quartz surface, it was proposed that the molecules were adsorbed through hydrogen bonding of the lone pairs of the nitrogen on the imidazole/imidazolium ring to the surface hydroxyl groups or from ion-dipole type interactions between the ionic liquids and the quartz surface.[12] The ionic liquids and neutral molecules form weak hydrogen bonds between the nitrogen atoms of the imidazole/imidazolium ring and surface silanol OH groups, as has been reported for other molecules with similar structures.[38,39]

It is apparent by comparing the spectra of [BMIM][BF_4] with [BMIM][PF_6] (Figures 4 and 5) that the relative antisymmetric methyl intensity is larger for [BMIM][BF_4] and that the anion has some influence on the orientation of the methyl group. [BMIM][BF_4] is miscible with water while [BMIM][PF_6] is not, and since they have the same cation, it is considered that the $[PF_6]^-$ anion is more hydrophobic than the $[BF_4]^-$ anion.[1] The

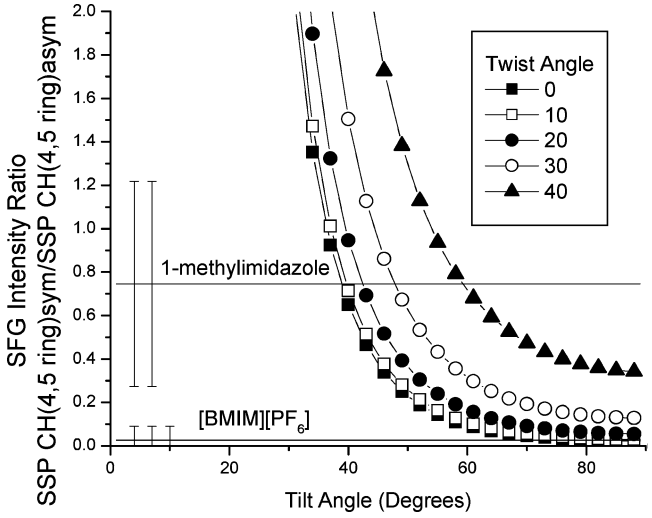

Figure 7. Simulation of SFG signal as a function of ring mode orientation of liquid/hydrophobic quartz interface.

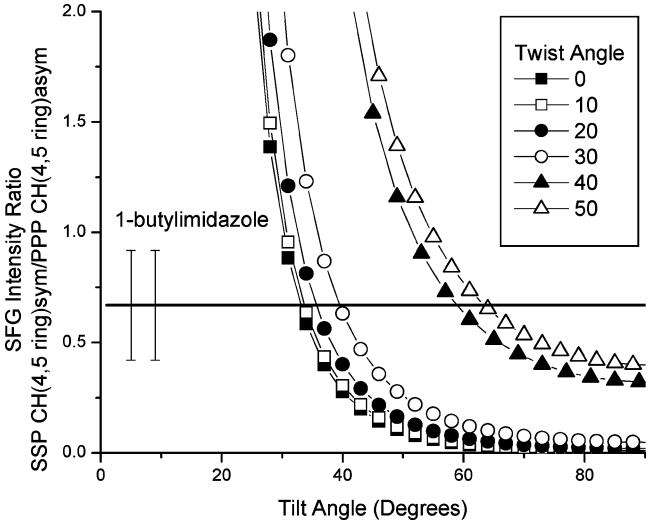

Figure 8. Simulation of SFG signal as a function of ring mode orientation of liquid/hydrophobic quartz interface.

more hydrophobic anion, $[PF_6]^-$, will have greater attraction to the nonpolar silane monolayer, while the hydrophilic anion, $[BF_4]^-$, will be more attracted to the polar C(2)−H group on the imidazolium ring. There is evidence for hydrogen bonding between the C(2) hydrogen and the anion for [BMIM][Cl], another water-miscible ionic liquid.[40,41] This difference in hydrophobicity of the anion is likely the cause of the difference in orientation of the methyl group for the two ionic liquids. The orientation of the methyl group is only mildly affected for the two ionic liquids because the anion must be close to the cation ring because of columbic interactions.

Calculation of the orientation of the imidazole/imidazolium ring is not as straightforward as for the methyl group. The imidazole/imidazolium ring is assigned C_{2v} symmetry. Free rotation around the symmetry axis of the ring cannot be assumed, unlike for the methyl group, because the imidazole/imidazolium ring cannot rotate around its C_2 symmetry axis if the molecule assumes a particular orientation. This produces orientation curves which are a function of both the tilt of the imidazole/imidazolium ring from surface normal and twist around the molecular symmetry axis. The low signal level of the C−H ring modes also increased the error associated with the intensity ratios, producing a wide range of possible tilt and twist angles.

The tilt angle of the ring mode of 1-methylimidazole was determined from Figure 7. The ratio of symmetric versus antisymmetric ring stretches from the ssp polarization combination was chosen to determine the orientation because of the level of signal to noise. This produced a tilt angle of 35−90° with 0−40° of twist. The large ambiguity of this measurement is due to all the possible twist orientations. If we constrain the possible twist angles of the imidazole ring to 0−30°, because of steric hindrance of the imidazole ring, the tilt of the imidazole ring becomes constrained to 35−63° from surface normal.

For 1-butylimidazole only, the symmetric ring mode was visible in the ssp polarized spectra and the antisymmetric ring vibration was observed in the ppp polarized spectra. The ratio of the intensities for these vibrations is shown in Figure 8. This curve predicts that the orientation of the imidazole ring for 1-butylimidazole is 31−82° with 0−50 ° of twist. As with 1-methylimidazole, if we constrain the possible twist angles of the imidazole ring to 0−30°, because of steric hindrance of the imidazole ring, the tilt of the imidazole ring becomes constrained to 31−44° from surface normal.

Only the antisymmetric H−C(4)C(5)−H ring mode was visible in the ssp and ppp polarizations for $[BMIM][BF_4]$. Therefore, the tilt angle of the ring was estimated to be 70−90° from normal, almost parallel to the surface.

For $[BMIM][PF_6]$, the symmetric and antisymmetric ring modes are only visible in the ssp polarized spectra. The intensity ratio is plotted versus the theoretical orientation curves in Figure 7. The calculated orientation is 60−90° with a possible twist of 0−20°.

The orientation of the imidazole ring of the neutral molecules is believed to be influenced by π-stacking of the absorbed molecules and by van der Waals interactions between terminal methyl groups or the monolayer and solvent, respectively. The face-to-face orientation of the methyl from the monolayer and those from the liquid has been observed previously in SFG experiments.[38,42,43] This creates a well-ordered system with the methyl groups (of the liquid-phase species) in a bilayer arrangement with the alkyl chain of the silane monolayer, and the imidazole rings are stacked to allow the maximum amount of molecules to interact with the silane monolayer.

For the ionic liquids, the orientation of the imidazolium ring is likely due to influence of the anion. If the anion did not have any influence on orientation, the ionic liquids would be oriented similar to 1-butylimidazole. Because the rings are charged and there are anions present, the rings cannot π stack as effectively as the neutral molecules.[41] This suggests that there are a wide variety of possible conformations of the cation ring. The weak intensity of the resonances from the imidazolium ring suggests that the ring is oriented in the plane of the surface. Because the ionic liquids are oriented with the methyl group toward the silane monolayer, the conformation of the imidazolium ring is not as constrained as on the hydrophilic quartz surface since the charge is not directly interacting with the surface.

Comparison of Imidazolium-Based Ionic Liquids with Ionic Surfactants. These results for ionic liquids at hydrophilic and hydrophobic quartz interfaces closely resemble the adsorption properties of ionic surfactants at both the air/water and quartz/water interfaces. The amphiphilic nature of imidazolium-based cations suggests that they could have similar interfacial behavior to the cations of ionic surfactants.[44] For ionic surfactants, the opposing interactions of the hydrophilic headgroup and hydrophobic tail with the surrounding media have been well studied.[20,45−48] When comparing the interfacial properties of ionic liquids to ionic surfactants, a key issue needs to be

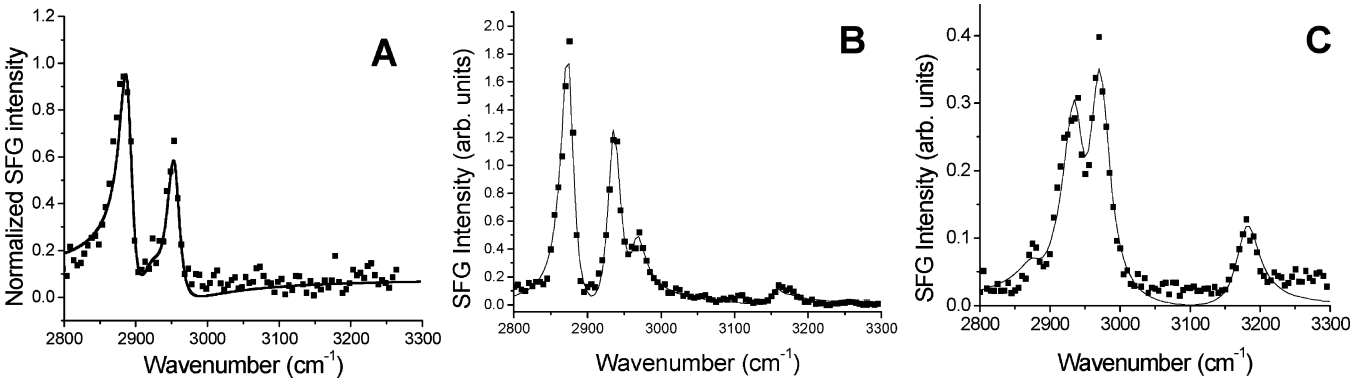

Figure 9. SFG spectra of [BMIM][PF_6] at three different interfaces ssp polarization (A) air/liquid, (B) hydrophobic quartz/liquid, and (C) hydrophilic quartz/liquid.

considered, the solvent. For ionic surfactants, the solvent can have an effect on molecular conformation.[20,48,49] Ionic liquids are pure ions, without solvent, so the molecular conformation is only due to intrinsic properties of the compound. Although the ionic liquids investigated in this study do not display a liquid-crystal phase,[50−52] the surface organization is driven by both the Coulombic interactions as well as the van der Waals forces.[53]

Comparison of Different Interfaces. Figure 9 shows the SFG spectra of [BMIM][PF_6] at three different interfaces: air/liquid, hydrophobic quartz/liquid, and hydrophilic quartz/liquid. The three spectra were recorded with the same incident angles. If air is assumed to be a nonpolar media and therefore the interface is hydrophobic, then it is possible to propose how ionic liquids absorb to hydrophilic and hydrophobic surfaces.

For hydrophobic surfaces, the methyl group from the alkyl chain of the cation is oriented toward the hydrophobic interface. As the surface becomes more hydrophobic, the methyl group is oriented more toward normal and the imidazolium ring lies in the plane of the surface. For the ionic liquid−air interface, studies have shown that the orientation of the cation is not dependent on the anion.[54] On the hydrophobic quartz surface, this is not the case. The orientation of the cation is influenced by the type of anion. The reason the anion influences the cation at the solid interface and not at the air interface is likely due to the difference in the surface energies for the alkyl chains at the two interfaces. The position of the anion was not probed in this study but it must remain close to the cation because of columbic interactions between the anion and the cation.

On hydrophilic surfaces, the ionic liquids and neutral molecules form weak hydrogen bonds between the nitrogen atoms of the imidazolium ring and surface silanol OH groups as well as hydrogen-bonding interactions with the charge centered on the aromatic ring. The anion also adsorbs to hydrophilic surfaces causing the cation to tilt toward the surface normal. The larger the anion, the more the cation is tilted from the surface.

Conclusions

SFG spectroscopy was used to characterize ionic liquids on a hydrophobic quartz interface. Two neutral compounds 1-methylimidazole and 1-butylimidazole were also examined to compare the ionic liquids to similar molecules. Deuterated dodecyltrichlorosilane was synthesized to modify a quartz surface, making it hydrophobic. The methyl group of each molecule studied was oriented toward the silane monolayer. The anion has an effect on both the orientation of the methyl group as well as the imidazolium ring. The imidazolium rings of the ionic liquids are believed to be lying in the plane of the interface. This study provides a direct in-situ observation that [BMIM]-[PF_6] and [BMIM][BF_4] can have different conformations at different interfaces.

Acknowledgment. This work was supported by grants from the Robert A. Welch Foundation (E1531), United States Air Force, and Universal Energy Systems. We thank R.K. Thomas for his advice with synthesis of deuterated silane. T.R.L. gratefully acknowledges support from the National Science Foundation (DMR-0447588) and the Robert A. Welch Foundation (E-1320).

Supporting Information Available: SFG orientation calculation. This material is available free of charge via the Internet at http://pubs.acs.org.

References and Notes

(1) Sheldon, R. *Chem. Commun.* **2001**, 2399−2407.
(2) Baldelli, S. *J. Phys. Chem. B* **2003**, *107*, 6148−6152.
(3) Fitchett, B. D.; Conboy, J. C. *J. Phys. Chem. B* **2004**, *108*, 20255−20262.
(4) Rivera-Rubero, S.; Baldelli, S. *J. Phys. Chem. B* **2004**, *108*, 15133−15140.
(5) Rivera-Rubero, S.; Baldelli, S. *J. Am. Chem. Soc.* **2004**, *126*, 11788−11789.
(6) Iimori, T.; Iwahashi, T.; Ishii, H.; Seki, K.; Ouchi, Y.; Ozawa, R.; Hamaguchi, H.; Kim, D. *Chem. Phys. Lett.* **2004**, *389*, 321−326.
(7) Solutskin, E.; Ocko, B. M.; Taman, L.; Kuzmenko, I.; Gog, T.; Deutsch, M. *J. Am. Chem. Soc.* **2005**, *127*, 7796−7804.
(8) Watson, P. R.; Gannon, T. J.; Law, G.; Carmichael, A. J.; Seddon, K. R. *Langmuir* **1999**, *15*, 8429.
(9) Watson, P. R.; Law, G. *Chem. Phys. Lett.* **2001**, *345*, 1.
(10) Katayanagi, H.; Hayashi, S.; Hamaguchi, H.; Nishikawa, K. *Chem. Phys. Lett.* **2004**, *392*, 460.
(11) Bowers, J.; Vergara, M. C.; Webster, J. R. P. *Langmuir* **2004**, *20*, 309−312.
(12) Romero, C.; Baldelli, S. *J. Phys. Chem. B* **2006**, *110*, 6213−6223.
(13) Ulman, A. *Chem. Rev.* **1996**, *96*, 1533−1554.
(14) Liu, Y.; Wolf, K.; Messmer, M. C. *Langmuir* **2001**, *17*, 4329−4335.
(15) Lagutchev, A. S.; Song, K. J.; Huang, J. Y.; Yang, P. K.; Chuang, T. J. *Chem. Phys.* **1998**, *226*, 337−349.
(16) Ye, S.; Nihonyanagi, S.; Uosaki, K. *Phys. Chem. Chem. Phys.* **2001**, *3*, 3463−3469.
(17) Hirose, C.; Akamatsu, N.; Domen, K. *J. Chem. Phys.* **1992**, *96*, 997−1004.
(18) Hirose, C.; Akamatsu, N.; Domen, K. *Appl. Spectrosc.* **1992**, *46*, 1051−1072.
(19) Hirose, C.; Yamamoto, H.; Akamatsu, N.; Domen, K. *J. Phys. Chem.* **1993**, *97*, 10064−10069.
(20) Bain, C. D. *J. Chem. Soc., Faraday Trans.* **1995**, *91*, 1281−1296.
(21) Fragneto, G.; Lu, J. R.; McDermott, C.; Thomas, R. K. *Langmuir* **1996**, *12*, 477−486.
(22) Fadeev, A. Y.; McCarthy, T. J. *Langmuir* **2000**, *16*, 7268−7274.
(23) MacPhail, R. A.; Strauss, H. L.; Elliger, C. A.; Snyder, R. G. *J. Phys. Chem.* **1984**, *88*, 334−341.

(24) Lu, R.; Gan, W.; Wu, B.-H.; Zhang, Z.; Guo, Y.; Wang, H.-F. *J. Phys. Chem. B* **2005**, *109*, 14118−14129.
(25) Carter, D. A.; Pemberton, J. E. *J. Raman Spectrosc.* **1997**, *28*, 939−946.
(26) Perchard, C.; Novak, A. *Spectrochim. Acta, Part A* **1967**, *23*, 1953−1967.
(27) Zhu, X. D.; Suhr, H.; Shen, Y. R. *Phys. Rev. B* **1987**, *35*, 3047−3050.
(28) Wang, H.-F.; Gan, W.; Lu, R.; Rao, Y.; Wu, B.-H. *Int. Rev. Phys. Chem.* **2005**, *24*, 191−256.
(29) Bunker, P. R. *Molecular Symmetry and Spectroscopy*; Academic: New York, 1970.
(30) Wilson, E. B.; Decius, J. C.; Cross, P. C. *Molecular Vibrations*; McGraw-Hill: New York, 1955.
(31) Demtroder, W. *Laser Spectroscopy*; Springer: New York, 1996.
(32) McHale, J. L. *Molecular Spectroscopy*; Prentice Hall: New Jersey, 1999.
(33) Skoog, D. A.; Holler, F. J.; Nieman, T. A. *Principles of Instrumental Analysis*, 5th ed.; Saunders College: Fort Worth, TX, 1998.
(34) Liu, J.; Conboy, J. C. *J. Am. Chem. Soc.* **2004**, *126*, 8894−8895.
(35) Liu, J.; Conboy, J. C. *J. Am. Chem. Soc.* **2004**, *126*, 8376−8377.
(36) Doyle, A. W.; Fick, J.; Himmelhaus, M.; Eck, W.; Graziani, I.; Prudovsky, I.; Grunze, M.; Maciag, T.; Neivandt, D. J. *Langmuir* **2004**, *20*, 8961−8965.
(37) Chen, C.; Even, M.; Wang, J.; Chen, Z. *Macromolecules* **2002**, *35*, 9130−9135.
(38) Liu, D.; Ma, G.; Allen, H. C. *Environ. Sci. Technol.* **2005**, *39*, 2025−3032.
(39) Dines, T. J.; MacGregor, L. D.; Rochester, C. H. *Spectrochim. Acta, Part A* **2003**, *59*, 3205−3217.
(40) Saha, S.; Hayashi, S.; Kobayashi, A.; Hamaguchi, H. *Chem. Lett.* **2003**, *32*, 740−741.
(41) Downard, A.; Earle, M. J.; Hardacre, C.; McMath, S. E. J.; Nieuwenhuyzen, M.; Teat, S. J. *Chem. Mater.* **2004**, *16*, 43−48.
(42) Johnson, M.; Leygraf, C.; Tyrode, E.; Rutland, M.; Baldelli, S. *J. Phys. Chem. B* **2005**, *109*, 329.
(43) Gan, W.; Wu, B. H.; Chen, H.; Guo, Y.; Wang, H. F. *Chem. Phys. Lett.* **2005**, *406*, 467.
(44) Bowers, J.; Butts, C. P.; Martin, P. J.; Vergara, M. C.; Heenan, R. K. *Langmuir* **2004**, *20*, 2191−2198.
(45) Conboy, J. C.; Messmer, M. C.; Richmond, G. L. *Langmuir* **1998**, *14*, 6722−6727.
(46) Sakai, K.; Torigoe, K.; Esumi, K. *Langmuir* **2001**, *17*, 4973−4979.
(47) Bain, C. D.; Davies, P. B.; Ward, R. N. *Langmuir* **1994**, *10*, 2060.
(48) Tanford, C. *The Hydrophobic Effect: Formation of Micelles and Biological Membranes*; Wiley-Interscience: New York, 1976.
(49) Casson, B. D.; Bain, C. D. *J. Phys. Chem. B* **1999**, *103*, 4678−4686.
(50) Gordon, C. M.; Holbrey, J. D.; Kennedy, A. R.; Seddon, K. R. *J. Mater. Chem.* **1998**, *8*, 2627.
(51) Holbrey, J. D.; Seddon, K. R. *J. Chem. Soc., Dalton Trans.* **1999**, *13*, 2133.
(52) Wei, X.; Hong, S. C.; Zhuang, X.; Goto, T.; Shen, Y. R. *Phys. Rev. E* **2000**, *62*, 5160.
(53) Binnemans, K. *Chem. Rev.* **2005**, *105*, 4148.
(54) Rivera-Rubero, S.; Baldelli, S. *J. Phys. Chem. B* **2006**, *110*, 4756−4765.